I J C T A, 10(9), 2017, pp. 583-591 ISSN: 0974-5572

A novel approach to MRI Brain Tumor delineation with Independent Components & Finite Generalized Gaussian Mixture Models

Megha Maria Cheriyan[1]*, Prawin Angel Michael[1] and Anil Kumar[2]

ABSTRACT

Automated segmentation of tumors from a multispectral data set like that of the Magnetic Resonance Images (MRI) is challenging. Independent Component Analysis (ICA) and its variations for Blind Source Separation (BSS) have been employed in previous studies but have met with cumbersome obstacles due to its inherent limitations. Here we have approached the multispectral data set initially with feature extraction followed by a kernel shape based unsupervised classification method, Finite Generalized Gaussian Mixture Model (FGGM) - ICA-FGGM model, for an improved classification of brain tissues in MRI. First, ICA is applied to MRI brain data from 3 source image sets - T1, T2 and PD/ FLAIR images to get optimally feature extracted three independent components. FGGM model can then incorporate various distributions from peaked ones to flat ones; thereby overriding the disadvantages of conventional approaches trying to represent data using a single probability density function. Expectation-Maximization algorithm is used to estimate the model parameters. Experiments were carried out initially on synthetic image sets to validate the algorithm and then on normal and abnormal clinical multispectral MRI brain images. Comparative studies using quantitative and qualitative analysis against conventional approaches confirm the effectiveness and superiority of the proposed method.

***Index Terms*:** Classification, Expectation-Maximization, Finite Generalized Gaussian Mixtures, Global Relative Entropy, Independent Component Analysis, Magnetic Resonance Imaging.

1. INTRODUCTION

The shape, size and extent of the brain disorder and the relationship to its surrounding need to be determined by the radiologists and neurosurgeons for a proper diagnosis and planning of therapy. This can be achieved from the multispectral MRI sequences such as T1-weighted images, T2-weighted images, PD (Proton Density) weighted images, FLAIR (Fluid Attenuated Inversion Recovery) images, DWI (Diffusion Weighted Images), etc. acquired for a pre-specified number of slices. With this large amount of database collected by clinicians, it becomes a herculean task to outline the specific area of interest. In some cases, early signs of the disease are often subtle in appearance and can be easily missed. So an automated approach to classification of normal and abnormal brain regions assumes vital importance. A review on MRI brain tumor segmentation methods is presented in [1].

Unsupervised classification methods [2] like Finite Gaussian Mixture models [3] and Fuzzy C Means [4] have been extensively worked on with respect to MRI brain images. Mounira R. [5] and her team worked on the classification of brain tissues and detection of multiple sclerosis lesions by modeling the brain image using Gaussian mixtures whose parameters where estimated using EM algorithm. Recently, A. Boulmerka and M.S. Allili [6] have modeled MRI data as a Mixture of Generalized Gaussian (MoGG)

[1,2] Karunya University, Tamil Nadu, *Email: meghamaria81@gmail.com, prawin@karunya.edu*

[3] Institute of Radiology & Imaging Sciences, Kerala, *Email: anil.k@medall.in*

distributions. The outputs suggested that this approach seemed to be much better than recent state-of-the-art techniques. In the recent past, Independent Component Analysis (ICA) [7] and its extensions prior to segmentation were found to be producing better results than conventional segmentation methods. Many researchers have carried out experiments based on ICA combined with various classification methods following either supervised or unsupervised learning such as ICA- SVM [8], ICA-FCM [9], ICA-Kmeans [10], etc. for classification of brain and pathological tissues.

In this work we propose to employ ICA prior to classification of brain tissues with FGGM to inherit the merits of both second order and higher order statistics. This research work is based on the impracticability of modeling non-gaussian data on Gaussian Mixture Models and for achieving higher classification accuracy from multispectral data using higher order statistics. Each independent component (IC) is further processed. Lloyd-Max histogram quantization is performed on the IC for initial segmentation. We then model the image histogram of the IC using finite generalized gaussian mixture distribution. The Expectation-Maximization (EM) algorithm is used for estimation of the parameters that define the statistical properties of the distribution of the image regions. Experiments were conducted both on synthetic and real-time clinical images. Comparison of the proposed method and the traditional classification methods were carried out using quantitative and qualitative assessment.

The rest of this paper is organized in the following manner: Section 2 details out the proposed algorithm with its theory. The database used, experimental results from the study and the discussions drawn from it are presented in Section 3. Section 4 concludes the paper and enlightens the reader with perspectives of possible future work.

2. ICA-FGGM MODEL

2.1. Independent Component Analysis

Independent Component Analysis was developed based on the principle of the cocktail-party problem [11]. The mathematical form of ICA [12] is expressed as in (1),

$$x = As \tag{1}$$

where x represents $\{x_1, x_2, ..., x_m\}^T$, the m-dimensional vector of the observed data, s represents $\{s_1, s_2, ..., s_n\}^T$, the n-dimensional vector of the source signals and A is an $m \times n$ mixing matrix. The ICs or the source signals can be estimated using the separating matrix W as in (2),

$$y = Wx, \text{ where } W = A^{-1} \tag{2}$$

Fast ICA [13] algorithm is applied on m-dimensional multispectral MR image set to extract 'n' classes consisting of brain tissues/ lesions. In this work, FastICA algorithm is applied on *3*-dimensional multispectral MR image set (T1, T2, PD/ FLAIR) to extract '3' ICs consisting of normal brain tissues and lesions.

2.2. Initial Segmentation using Lloyd-Max Quantization

Each IC can be coarsely quantized using a multilevel thresholding method called Self-Organizing Lloyd-Max Quantizer [14]. This method is insensitive to effects of noise. The algorithm also carries the advantage of not having any prior knowledge of the image histogram.

2.3. Finite Generalized Gaussian Mixture Model

The FGGM model [15] is a generalization of the widely used Gaussian Mixture Model that can accommodate sub and super-gaussian distributions. Consider an MRI brain image having $N_1 \times N_2$ pixels to have K classes. By treating pixel labels as random variables and considering π_k as a measure of prior probability of the k^{th} initially quantized region equal to n_k/N (where $N = N_1 \times N_2$), the probability density function (pdf) of the FGGM model can be written as,

$$p(u_i) = \sum_{k=1}^{K} \pi_k p_k(u_i), i = 1, 2, ..., N \quad (3)$$

where N is the total count of pixels in the brain region and $u_i = 0, 1, ..., G-1$ is the grey level of the i^{th} pixel with G being the number of grey levels. $p_k(u_i)$ is the generalized Gaussian pdf defined by

$$p_k(u_i) = \frac{\alpha\beta_k}{2\tau(1/\alpha)} \exp\left[-\left|\beta_k(u_i - \mu_k)\right|^{\alpha}\right],$$

where

$$\alpha > 0, \beta_k = \frac{1}{\sigma_k}\left[\frac{\tau(3/\alpha)}{\tau(1/\alpha)}\right]^{1/2}. \quad (4)$$

With respect to the k^{th} region, μ_k is the mean of all grey level values, σ_k is its standard deviation and $\beta_k \propto 1/\sigma_k$. $\tau(.)$is the gamma function and α is the parameter that decides the kernel shape of the densities. For $\alpha = 2$, the pdf tends to be Gaussian. For $\alpha >> 1$, the pdf tends to be more uniform. For $\alpha < 1$, the pdf tends to be more sharper [16].

The parameter set s:$\{\alpha, \pi_k, \mu_k, \sigma_k\}$, k = 1, 2, ..., K that structures the model is estimated using the popular EM [15] algorithm. In this work, Global Relative Entropy (GRE) is used to achieve optimum parameter estimates and is given by,

$$GRE(p_u \; II \; p_s) = \sum_x p_u(x) \log \frac{p_u(x)}{p_s(x)} \quad (5)$$

where $p_u(x)$ is the histogram of the original image and $p_s(x)$ is the estimated probability measure of the grey levels in the image. The GRE value is computed for every iteration in the estimation process and finally the optimum parameter set $\hat{s}$ is selected for which the GRE is minimum. K and a are the important parameters in model selection. The value of K is selected by minimizing the Minimum Description Length (MDL) [17] value defined by,

$$MDL(K) = -\log\left(L(\hat{s}_{ML})\right) + 0.5K' \log(N) \quad (6)$$

where $\hat{s}_{ML}$ is the Maximum Likelihood estimate [15] of the parameter set s, L is the likelihood function and K′ is the number of parameters that can be adjusted in the set. The optimum value of K is achieved at the minima of the MDL curve,

$$K_{opt} = \arg\left\{\min_{1 \le K \le K_{MAX}} MDL(K)\right\} \quad (7)$$

Final segmentation is carried out using Lloyd-Max histogram Quantization with K_{opt} classes.

2.4. Proposed Algorithm

Step 1: Construct a multispectral image I by placing T1W image, T2W image and FLAIR/PD image in 1st, 2nd and 3rd dimension respectively.

Step 2: Apply FASTICA algorithm on I to generate three ICs - IC1, IC2 and IC3.

Step 3: For different values of K, repeat following for each IC,

3.1. Find initial thresholds for segmentation using Lloyd-Max algorithm.

3.2. Perform FGGM modeling on the image pdf using (3) and (4).

3.3. Estimate the parameters using EM algorithm iteratively.

Calculate GRE using (5) at every iteration.

If $abs(GRE(current) - (GRE(previous)) < \in$, break loop; else repeat.

3.4. Select optimal parameter set (n, μ, and σ) of model with minimum GRE.

Calculate pdf corresponding to FGGM using optimized parameters.

3.5. For each class K, find MDL(K) as given in (6).

3.6. Find 'K_{opt}' corresponding to minimum MDL value using (7).

3.7. Apply Lloyd-Max algorithm on estimated FGGM with K_{opt}.

Step 4: Output classified images using the newly generated thresholds.

3. EXPERIMENTS

3.1. Databases

The synthetic multispectral images of the brain were collected from BrainWeb [18]. T1-weighted image (T1WI), T2-weighted image (T2WI) and Proton density image (PDI) for normal brain and abnormal brain were included for our experiments. The ground truth database of various tissues of the brain were also available from the website. The parameters were set as slice thickness = 1mm, intensity non-uniformity = 0% and noise level = 0%.

The clinical multispectral images(T1WI, T2WI and FLAIR) of the brain were sampled by Siemens' whole body 3T MR system (Siemens, AG Medical Solutions, Erlangen, Germany). 50 cases defining tumors and normal brain tissues were considered in the study. The acquisition of the T1WI/ T2WI/ FLAIR were conducted as per the settings: TR(repetition time(ms))=1600/ 4000/ 7000; TE(echo time(ms))=8.9/ 95/ 94 respectively and TI(inversion time)=2026.5ms only for FLAIR. Slice thickness/slice gap were set as 5mm/ 6.5mm**.**

3.2. Results and Discussion

The proposed algorithm is applied on normal and abnormal brain MRI data set. The proposed method was implemented in MATLAB R2013a/Win 64 installed on an Intel Core 2 Quad Q9300 CPU with 2.5GHz speed and 4.00 GB RAM. As a pre-processing step to prepare multispectral data, clinical MR images were rotated and skewed using control point function in MATLAB to keep the alignment same among corresponding images. Further processing like de-noising and contrast enhancement were not carried out due to possibility of loss of information. The average values of mean and standard deviation of each class obtained using FGGM for three ICs are listed in Table 1.

Table 1
Average mean and standard deviation of various classes from ICs for the clinical image sets.

Class	*IC1+FGGM*		*IC2+FGGM*		*IC3+FGGM*	
	SD	*Mean*	*SD*	*Mean*	*SD*	*Mean*
1	6.28	5.60	5.02	4.82	9.18	6.23
2	7.58	24.99	6.53	16.69	13.52	44.11
3	11.67	44.19	10.31	41.30	12.35	79.16
4	23.30	109.07	13.30	76.45	10.77	124.90
5	26.42	193.04	15.61	124.43	22.19	152.46
6	27.52	286.47	14.65	198.61	30.42	188.94

Fig. 1 shows how the graph settles to its optimal K value during FGGM estimation for each IC. Initially K values were set as 6. After iterative estimation, these values were observed to be reducing to optimal values (for IC1 and IC2 - 5 classes and for IC3 - 6 classes).

Iterative estimation reduces the relative entropy between the image histogram and the estimated pdf to a minimum value at a faster rate for our proposed algorithm than the conventional one. This is graphically represented in fig. 2.

The experiments were conducted for the kernel shape parameter α = 1, 2, 3, 4. Li *et al.* [15] has determined in his experiments on real time digital mammograms that the GRE value is the least with $\alpha = 3$. In our experiments, we have also observed minimum GRE value for $\alpha = 3$. The significant reduction in information theoretic distance (GRE) between the histogram of the original image and the model's distribution after estimation is pictorially illustrated in fig. 3. Estimated pdf and image histogram are found to be more or less similar after parameter estimation.

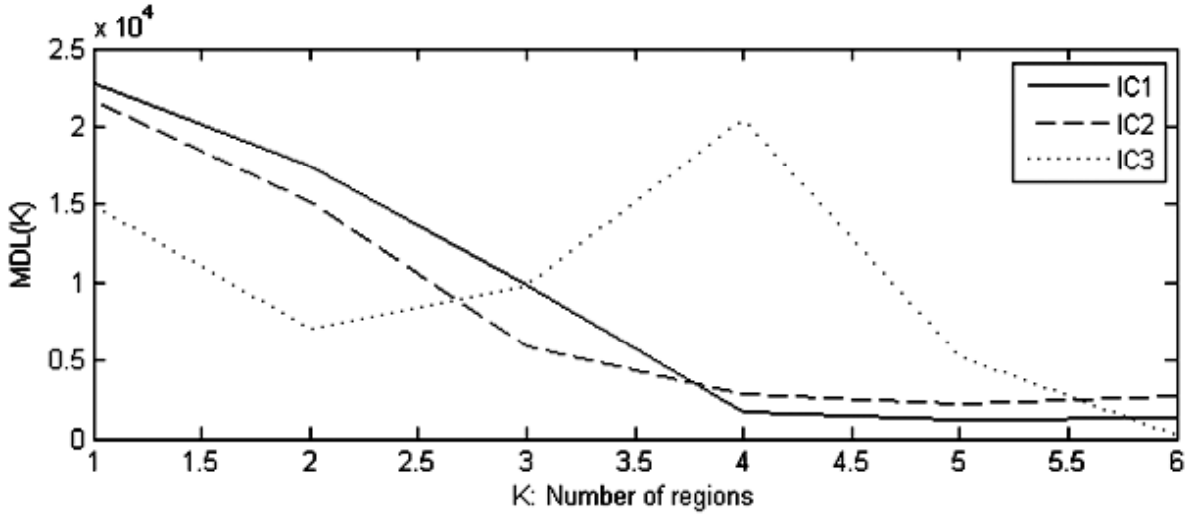

Figure 1: Finding optimal value of K using MDL for each IC.

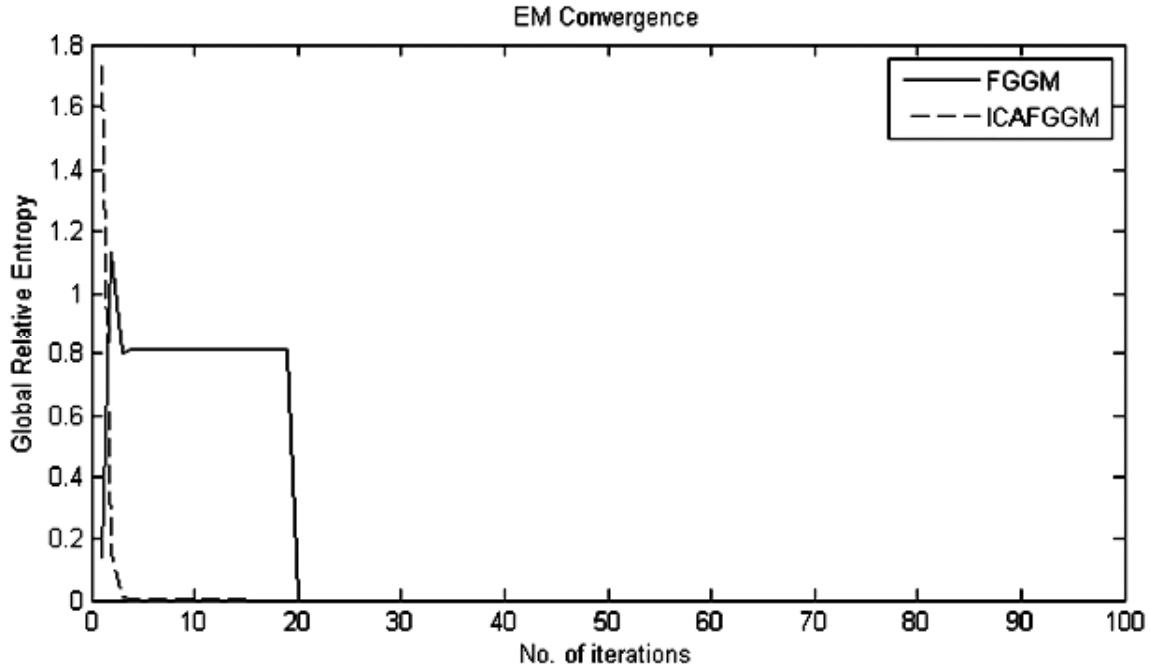

Figure 2: Graph showing GRE values of two consecutive iterations as it reaches maximum no. of iterations for FGGM and proposed algorithm.

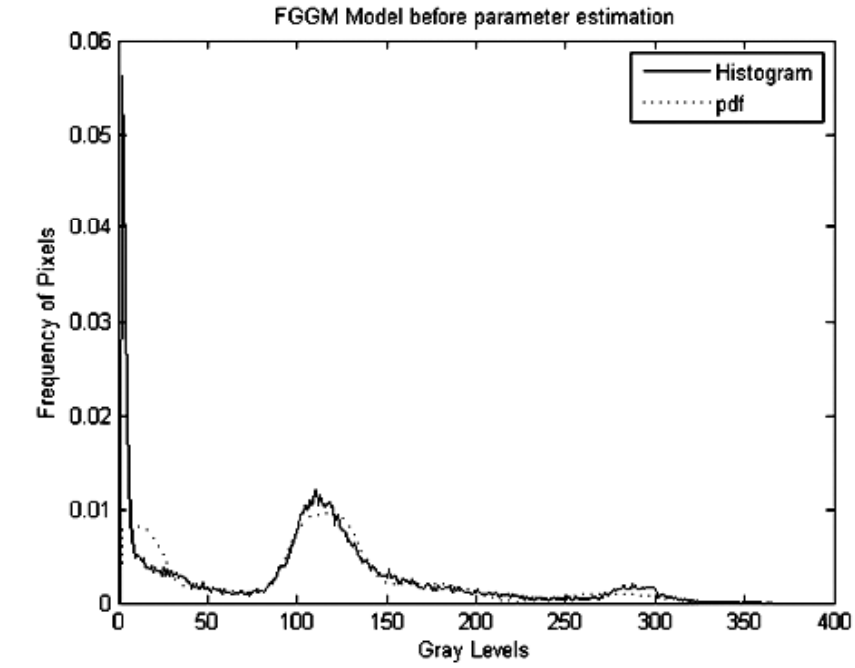

(a)

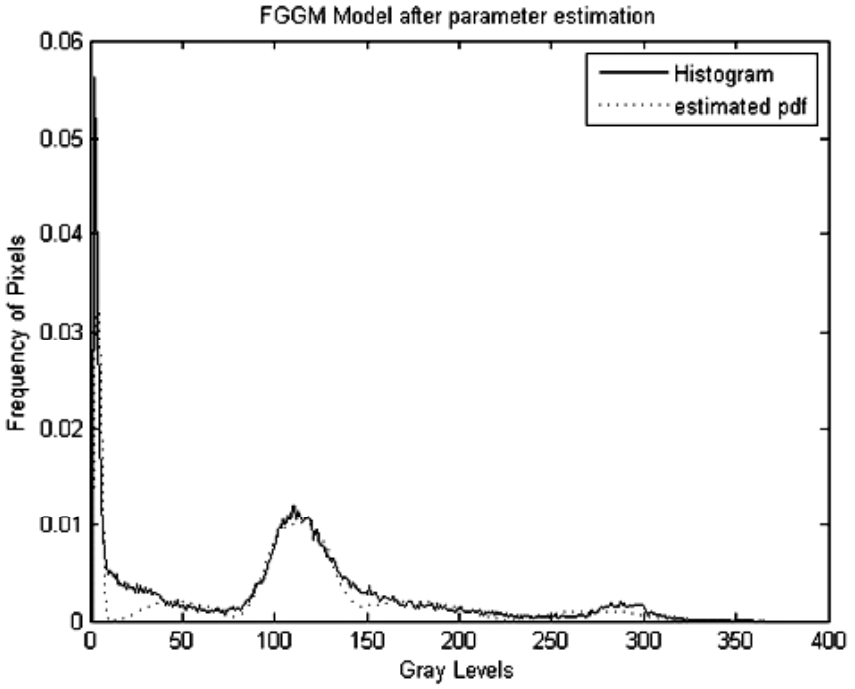

(b)

Figure 3: FGGM model of the clinical MRI image set: (a) before parameter estimation and (b) after parameter estimation using EM algorithm for one IC.

Fig. 4 illustrates an example of the visual results obtained from our experiments on the clinical image set under study. Proposed algorithm is found to be promising in the separation of White Matter (WM) accurately specifying abnormality locations. Abnormal cells are also found to be clearly distinguishable from the background. Such a differentiation was not achieved with the other algorithms.

In tumors with pockets of bleeding or tissue necrosis, the delineation of the WM pockets was not optimal when compared with ground truth from the radiologists but the inter-observer variability between various radiologists was also high.

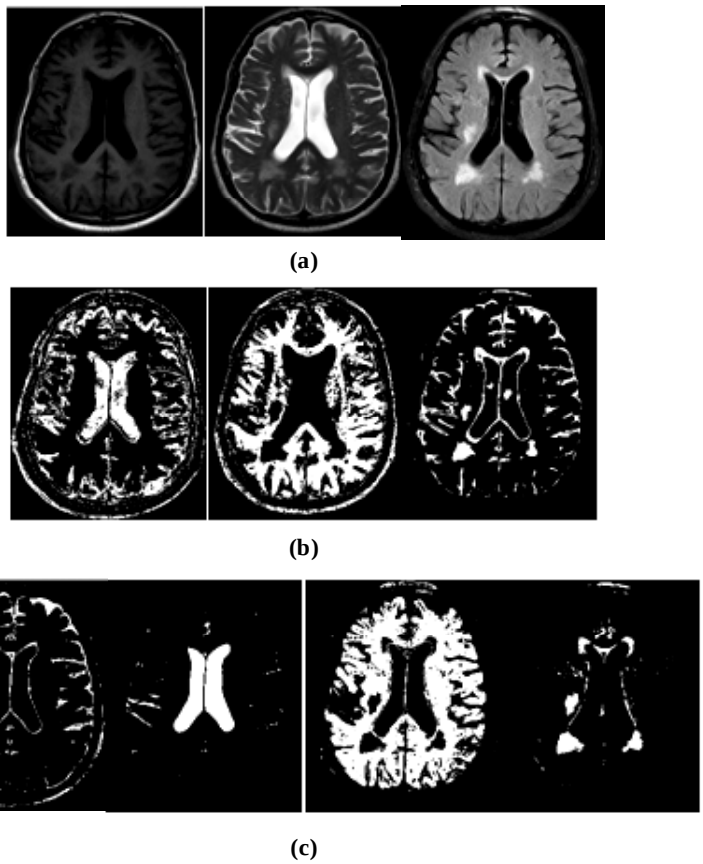

(a)

(b)

(c)

Figure 4: Results obtained with clinical MRI brain image (a) T1,T2, FLAIR images. (b) Classified images using FGGM-EM(without ICA) (c) Classified images of the ICs using FGGM-EM.

3.3. Performance Evaluation

The performance of our experiments is quantitatively evaluated using Tanimoto Index (TI) and other statistical measures like Specificity and Accuracy [8] using synthetic images. The average of these values for K-means, FCM, FGGM and the proposed method are tabulated in table 2 for comparative analysis. The

Table 2 Comparison of Performance Measure of different methods for Synthetic images for (a) WM and GM, and (b) Lesions.

	WM			*GM*		
	TI	*Sp*	*Acc*	*TI*	*Sp*	*Acc*
K-Means	0.87	0.94	0.96	0.60	0.88	0.90
FCM	0.89	0.98	0.97	0.64	0.92	0.91
FGGM	0.90	0.98	0.97	0.65	0.90	0.90
ICA-FGGM	0.96	0.99	0.99	0.63	0.89	0.90

(a)

	Lesions		
	TI	*Sp*	*Acc*
K-Means	0.58	0.86	0.90
FCM	0.53	0.91	0.90
FGGM	0.53	0.94	0.93
ICA-FGGM	0.64	0.99	0.99

(b)

average TIs of WM measurements of the ICA-FGGM method is 0.96 for the synthetic image data sets which is extremely higher than other conventional approaches. A very good improvement is also observed in the case of lesions. CSF details clustered together with tumor details produced lesser value of TI for conventional method compared to proposed method. Improved accuracy values observed for WM and lesions proved the robustness and efficiency of the algorithm especially in lesion detection.

A drastic decrease in execution time is also noted for proposed method when compared with the other algorithms. The averaged estimated times for different ICs are summarized in Table 3.

Table 3
Comparison of the computation time required for the proposed algorithm and conventional algorithm.

Time(in sec)	*IC1*	*IC2*	*IC3*
FGGM	309.2143	512.7774	62.2155
Proposed method	40.7428	15.2385	17.5667

4. CONCLUSION

In this paper, we propose an innovative ICA based FGGM modeling for enhancement and better classification of MRI brain tissues and lesions. The proposed method has been initially tested on synthetic images as proof of concept. Subsequent application on a varied range of clinical images from small homogenous lesions like Multiple Sclerosis to heterogeneous images of tumors have proved that the proposed algorithm has significant advantages over existing ones. Subjective (visual comparison by experts) and objective (quantitative) assessment has proved our initial observations. Improved Tanimoto index values for WM and lesions (0.96 and 0.64 respectively) are indications of image quality enhancement on application of ICA prior to a conventional classification using FGGM (0.90 and 0.53 respectively). Significantly reduced computational time for the proposed ICA-FGGM model also gives it an upper hand over conventional methods. Improving the optimization process with global or heuristic optimization methods can be looked into as a future work.

ACKNOWLEDGEMENT

The authors would like to thank Dr. Easter Selvan for the guidance given and Institute of Radiology and Imaging Sciences, Kochi for supporting the research work with clinical data.

REFERENCES

[1] K.P.S. Shijin, and V.S. Dharun, "A Study of MRI Segmentation Methods in Automatic Brain Tumor Detection," International Journal of Engineering Technology, vol.8, no.2, pp.609-614, Apr-May 2016.

[2] N. Sauwen, M. Acou, S.D.M. Van Cauter, D. M. Sima, J. Veraart, F. Maes, *et al.*, "Comparison of unsupervised classification methods for brain tumor segmentation using multi-parametric MRI,"NeuroImage: Clinical, vol.12, pp.753-764, Sep 2016.

[3] M.A. Balafar, "Fast and robust gaussian mixture model for MRI brain image segmentation,"International Journal on Technical and Physical Problems in Engineering, vol.5, no.2, pp. 8-14, June 2013.

[4] R. He, S. Datta, B.R. Sajja, and P.A. Narayana, "Generalized fuzzy clustering for segmentation of multi-spectral magnetic resonance images,"Computerized Medical Imaging and Graphics, vol. 32, pp. 353–366, Feb 2008.

[5] M. Rouainia and N. Doghmane, "Quantitative stochastic analysis of Magnetic Resonance images of the brain,"2nd International Conference on Information & Communication Technologies, Damascus, pp. 1785-1789, Oct 2006.

[6] A. Boulmerka, and M.S. Allili, "Thresholding-based segmentation revisited using mixtures of generalized gaussian distributions,"21st International Conference on Pattern Recognition, Tsukuba, pp. 2894-2897, Nov 2012.

[7] A. Hyvarinen, J. Karhunen, and E. Oja, "Independent Component Analysis," John Wiley and Sons, Mar 2001.

[8] S. Sindhumol, K. Anil, and B. Kannan, "Spectral clustering Independent Component Analysis for tissue classification from brain MRI," Biomedical Signal Processing and Control, vol. 8, pp .667-674, Nov 2013.

[9] Y-C. Ouyang, H-M. Chen, J-W. Chai, C. C-c. Chen, S-K. Poon, C-W. Yang, *et al.*, "Band expansion-based over-complete Independent Component Analysis for multispectral processing of Magnetic Resonance images," IEEE transactions on Biomedical Engineering, vol. 55, no. 6, pp. 1666-1677,June 2008.

[10] T. Tateyama, Z. Nakao, and Y. Chen, "Classification of Brain Matters in MRI by Kernel Independent Component Analysis," International Conference on Intelligent Information Hiding and Multimedia Signal Processing, pp.713-716, Aug 2008.

[11] P. Neha, "Independent Component Analysis for BCI system," International Journal of Technical Research and Applications, vol. 4, pp. 295-297, Mar-Apr 2016.

[12] C. Jutten, and J.Herault, "Blind separation of sources, Part I: an adaptive algorithm based on neuromimetic architecture," Signal processing, vol.24,pp.1-10, 1991.

[13] A. Hyvarinen, "Fast and robustfixed point algorithm for ICA," IEEE transactions on Neural Networks, vol. 10, pp. 626-634, 1999.

[14] Y. Wang, T. Adali, and B. Lo, "Automatic threshold selection by histogram quantization," Journal of Biomedical Optics, vol. 2, pp. 211-217, 1997.

[15] H. Li, Y. Wang, K.J.R. Liu,S.-C.B. Lo, and M.T. Freedman, "Computerized radiographic mass detection—Part I: Lesion site selection by morphological enhancement and contextual segmentation," IEEE Transactions on Medical Imaging, vol. 20, pp. 289–301, 2001.

[16] K.N. Kumar, K.S. Rao, Y. Srinivas, and Ch. Satyanarayana, "Studies on texture segmentation using D-Dimensional Generalized Gaussian distribution integrated with Hierarchical Clustering," International Journal of Image Graphics and Signal Processing, vol. 8, 45-54, 2016.

[17] J. Rissanen, "Modeling by shortest data description,"Automatica, vol. 14, pp. 465–471, 1978.

[18] http://brainweb.bic.mni.mcgill.ca/brainweb/